ORIGINAL RESEARCH
published: 10 November 2021
doi: 10.3389/fenrg.2021.769374

Simulation of Nanofluid Flow in a Micro-Heat Sink With Corrugated Walls Considering the Effect of Nanoparticle Diameter on Heat Sink Efficiency

Yacine Khetib[1,2]*, *Hala M. Abo-Dief*[3], *Abdullah K. Alanazi*[3], *Goshtasp Cheraghian*[4], *S. Mohammad Sajadi*[5,6] *and Mohsen Sharifpur*[7,8]*

[1]Mechanical Engineering Department, Faculty of Engineering, King Abdulaziz University, Jeddah, Saudi Arabia, [2]Center Excellence of Renewable Energy and Power, King Abdulaziz University, Jeddah, Saudi Arabia, [3]Department of Chemistry, College of Science, Taif University, Taif, Saudi Arabia, [4]Independent Researcher, Braunschweig, Germany, [5]Department of Nutrition, Cihan University-Erbil, Erbil, Iraq, [6]Department of Phytochemistry, SRC, Soran University, Soran, Iraq, [7]Department of Mechanical and Aeronautical Engineering, University of Pretoria, Pretoria, South Africa, [8]Department of Medical Research, China Medical University Hospital, China Medical University, Taichung, Taiwan

OPEN ACCESS

Edited by:
Cong Qi,
China University of Mining and Technology, China

Reviewed by:
Basharat Jamil,
Rey Juan Carlos University, Spain
Hossein Nasiri,
Brazil University, Brazil

***Correspondence:**
Yacine Khetib
ykhetib@yahoo.com
Mohsen Sharifpur
mohsen.sharifpur@up.ac.za

Specialty section:
This article was submitted to Process and Energy Systems Engineering, a section of the journal Frontiers in Energy Research

Received: *01 September 2021*
Accepted: *23 September 2021*
Published: *10 November 2021*

Citation:
Khetib Y, Abo-Dief HM, Alanazi AK, Cheraghian G, Sajadi SM and Sharifpur M (2021) Simulation of Nanofluid Flow in a Micro-Heat Sink With Corrugated Walls Considering the Effect of Nanoparticle Diameter on Heat Sink Efficiency. Front. Energy Res. 9:769374. doi: 10.3389/fenrg.2021.769374

In this numerical work, the cooling performance of water–Al_2O_3 nanofluid (NF) in a novel microchannel heat sink with wavy walls (WMH-S) is investigated. The focus of this article is on the effect of NP diameter on the cooling efficiency of the heat sink. The heat sink has four inlets and four outlets, and it receives a constant heat flux from the bottom. CATIA and CAMSOL software were used to design the model and simulate the NF flow and heat transfer, respectively. The effects of the Reynolds number (*Re*) and volume percentage of nanoparticles (Fi) on the outcomes are investigated. One of the most significant results of this work was the reduction in the maximum and average temperatures of the H-S by increasing both the *Re* and Fi. In addition, the lowest T_{max} and pumping power belong to the state of low NP diameter and higher Fi. The addition of nanoparticles reduces the heat sink maximum temperature by 3.8 and 2.5% at the Reynolds numbers of 300 and 1800, respectively. Furthermore, the highest figure of merit (FOM) was approximately 1.25, which occurred at *Re* = 1800 and Fi = 5%. Eventually, it was revealed that the best performance of the WMH-S was observed in the case of *Re* = 807.87, volume percentage of 0.0437%, and NP diameter of 20 nm.

Keywords: heat sink, electronic component, nanoparticles diameter, alumina–water nanofluid, numerical simulation

INTRODUCTION

Advances in technology and electronic devices have posed a formidable challenge for related industries. Increasing the power of electronic devices in many cases causes them to heat up; in some cases it reduces the performance of the devices and, in certain circumstances, causes the electronic devices to fail. Hence, it is of absolute necessity to cool this equipment properly. The application of electronic equipment in devices such as cellphones and tablets in a small space has caused heat transfer to occur in a tiny space. CPUs are one of these electronic devices and cooling them is required in all of the abovementioned devices. As their computing power enhances, the generated

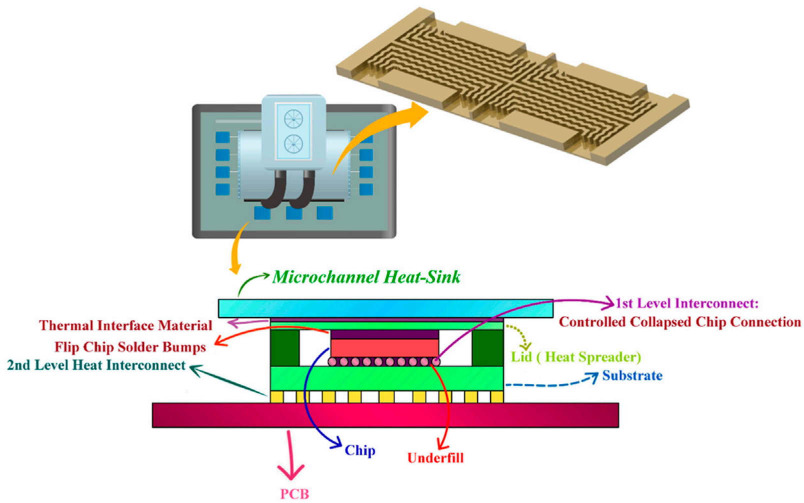

FIGURE 1 | General scheme of the problem.

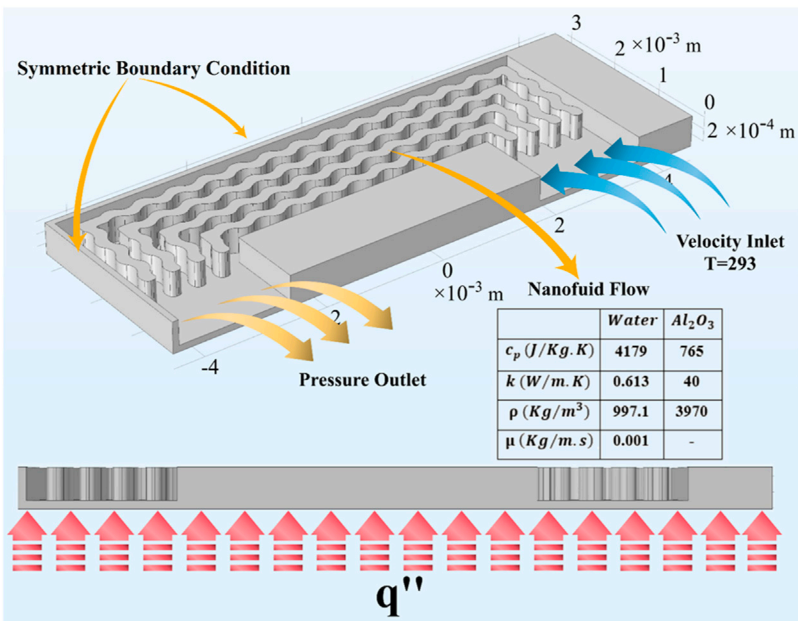

	$Water$	Al_2O_3
$c_p\ (J/Kg.K)$	4179	765
$k\ (W/m.K)$	0.613	40
$\rho\ (Kg/m^3)$	997.1	3970
$\mu\ (Kg/m.s)$	0.001	-

FIGURE 2 | Boundary conditions applied to the problem geometry and thermophysical properties of H_2O and Al_2O_3 NPs.

heat increases, and as a result, they need to be cooled down by heat sinks (H-Ss) to prevent the reduction in their performance (Ghani et al., 2017; Sohel Murshed and Nieto de Castro, 2017; Bahiraei and Heshmatian, 2018a; Ahmed et al., 2018; Pordanjani et al., 2021). Owing to the tiny size of the CPUs, it is necessary to employ micro-heat sinks (MH-Ss) in this regard. In MH-Ss, the fluid flows in the microchannels and cools the H-S and consequently the electronic equipment. The growing needs of industries for MH-Ss with increased cooling capacities has led to an increment in studies in recent decades (Tullius et al., 2011; Shalchi–Tabrizi and Seyf, 2012; Mohammed Adham et al., 2013; Sohel et al., 2015; Kumar et al., 2018). So far, particularly in recent years, several researchers have conducted various studies on the analysis of cooling devices (Bagherzadeh et al., 2019; Ahmadi et al., 2020a; Peng et al., 2020; Shadloo et al., 2020; Safdari Shadloo, 2021). In one of these studies, Kumar and Singh (2019) numerically inspected the influence of inlet and outlet on the thermal performance of an H-S. They studied an H-S comprising some parallel microchannels and utilized H_2O to cool it. Their simulation results demonstrated that augmenting the *Re*

TABLE 1 | Average temperature changes of heat sink for different elements at Re = 300 for Fi = 5%.

Number of Meshes×10^{-3}	370	980	1,145	1,310	1,550	1820	2014
Heat sink average temperature	306.89	304.55	303.31	302.44	301.95	301.93	301.93

TABLE 2 | Average Nusselt number along the channel for the present work and Ho and Chen (2013).

Re	135	390	655	915	1,300	1,530
Ho and Chen (2013)	6.07	7.71	10.12	12.14	13.15	13.63
Present work	5.88	7.43	9.72	11.83	12.82	13.43
%Err	3.1	3.6	3.9	2.5	2.5	1.4

raises the pressure drop (ΔP) in the H-S. Furthermore, they also found that increasing the volumetric flow rate of the fluid decreased the thermal resistance of the H-S.

In general, researchers have used both numerical and experimental methods for their studies in the field of fluid mechanics (Kalbasi et al., 2019; Guan et al., 2020; Hu et al., 2020; Giwa et al., 2021; Hu et al., 2021). The use of experimental methods is reliable, but costly. In many numerical studies, validation has been done by the comparison of the numerical results with experimental data, and as a result, experimental work has been expanded (Esfe et al., 2018; Hemmat Esfe et al., 2018; Bahrami et al., 2019; Pordanjani et al., 2019; Zheng et al., 2020). Numerical research is less expensive than laboratory work and can be done in less time (Afrand et al., 2014; Osman et al., 2019; Ahmadi et al., 2020b; Sokhal et al., 2021).

In a myriad of conducted studies, NFs have been used to cool down different types of heat devices (Aybar et al., 2015; Ghodsinezhad et al., 2016; Sharifpur et al., 2016; Awais and Kim, 2020; Irandoost Shahrestani et al., 2020). NFs exhibit higher thermal conductivity than simple fluids (Toghyani et al., 2019; Vahedi et al., 2019; Ghalandari et al., 2020; Yan et al., 2020; Pordanjani and Aghakhani, 2021). Numerous articles have recommended the application of nanotechnology in the industry (Hajatzadeh Pordanjani et al., 2019; Zhang et al., 2020; Handschuh–Wang et al., 2021; Tian et al., 2021; Wang et al., 2021). In this regard, studies by Ambreen and Kim (2020), Wu et al. (2016), Alfaryjat et al. (2018), and Arani et al. (2017) can be referred. In one of these research studies, Bahiraei and Heshmatian (2018b) examined the influence of the presence of hybrid NFs on the performance of a rectangular H-S. They examined a heat sink comprising four similar sections, each containing five microchannels ,and a fixed thermal flux of 100 W/cm^2 applied on the bottom of the H-S. Their simulation results demonstrated that increasing the NF velocity from 1 to 3 m/s decreased the T_{Max} of the H-S to approximately 313 K. However, they indicated that increasing the velocity greatly increased the power required to pump the fluid. In several studies, wavy walls have been used instead of smooth walls for micro-channels. Using this type of wall can enhance heat transfer (Arani et al., 2017; Nguyen et al., 2019; Alihosseini et al., 2020).

Nanoparticles (NPs) can be made in different dimensions in nanoscale. Many NPs have different dimensions. Alumina NPs, one of the most widely used NPs, are produced in various dimensions. The dimensions of the NPs can affect the thermal conductivity and viscosity of the NF. However, few researchers have considered the effect of the NP diameter on heat transfer, especially in heat sinks. Owing to the importance of cooling electronic devices, particularly CPUs in various functional devices, this article numerically studied a new H-S. This H-S had four similar sections where the fluid entered through 4 inlets and exited out of 4 outlets. In order to improve heat transfer, NFs were employed for cooling, and microchannels with wavy walls (WW) were also considered. The model used for single-phase viscosity and thermal conductivity also depended on the diameter of the nanoparticles (NPs),and its influence on the thermal performance of the WW in H-S has also been investigated. An innovation of this study is to use wavy channel walls in the heat sink and to assess the effect of the nanoparticle diameter on the thermal efficiency of a heat sink .

PROBLEM DEFINITION

The studied WMH-S, presented in **Figure 1**, had four inlets and four outlets. This aluminum WMH-S comprised of four similar sections. The height of the WMH-S was 0.5 mm and its overall dimension was 18 × 6.2 mm. The dimensions of the heat sink inlet are 1.8 mm, and the height of microchannels is 0.4 mm. A 0.2-mm-thick aluminum door is placed on the heat sink. Within the WMH-S, nanomaterials, Al_2O_3/H_2O NF with volume percentages ranging from 0 to 5% flowed in a *Re* of 300, 800, 1,300, and 1,800. A constant heat flux, from the operation of an electronic device, was applied on the bottom of the WMH-S. The aluminum used in the heat sink has a thermal conductivity of 179.96 W/m.K, a density of 2,712.6 kg/m^3, and a heat capacity of 0.96 kJ/kg K (Kant et al., 2017).

GOVERNING EQUATIONS

The general equations governing the fluid flow within the H-S in the single-phase form are as follows. These equations include the conservation of mass, momentum, and energy. The fluid flow is laminar and steady, and the fluid is an incompressible Newtonian (Akbari et al., 2011).

$$\nabla.\left(\rho\vec{v}\right) = 0, \tag{1}$$

$$\rho\vec{v}.\nabla\vec{v} = -\nabla P + \nabla.\left(\mu\nabla\vec{v}\right), \tag{2}$$

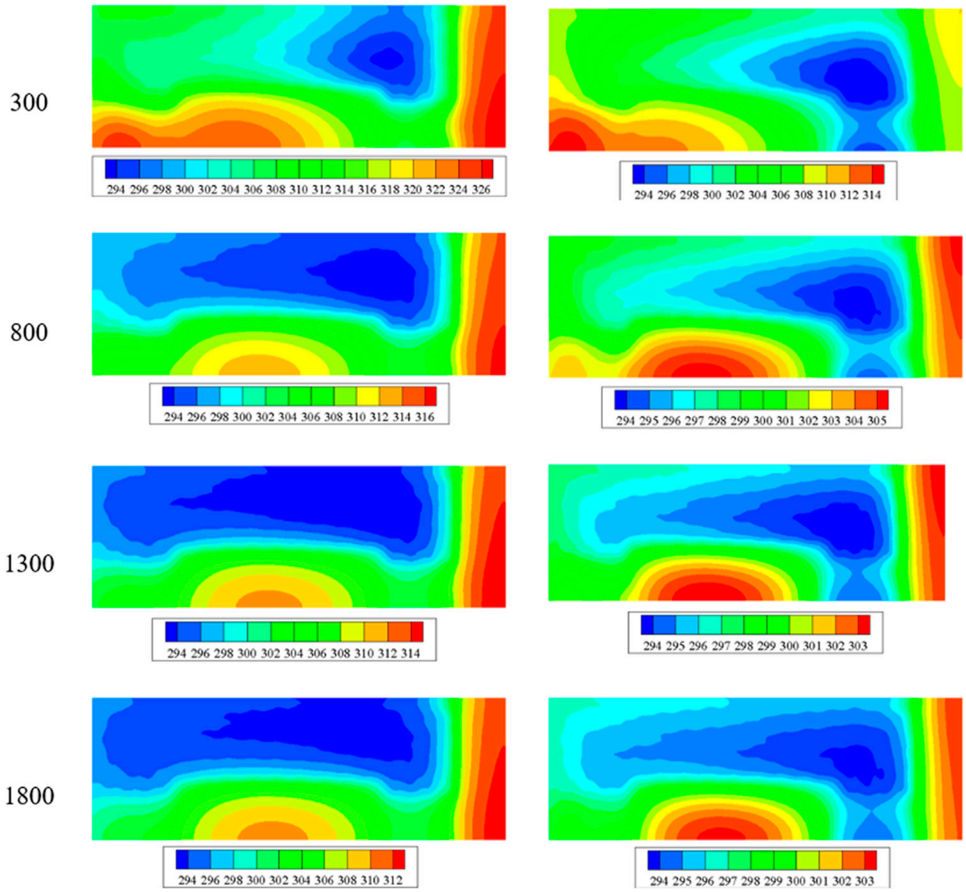

FIGURE 3 | Temperature contour of the H-S in for H_2O and NF 2% in dissimilar Re.

$$\nabla.\left(\rho\vec{v}c_pT\right) = \nabla.\left(k\nabla \mathrm{T}\right), \tag{3}$$

$$0 = \nabla.\left(k_{\mathrm{aluminum}}\nabla \mathrm{T}\right), \tag{4}$$

where $\vec{v}$, T, and P are velocity, temperature, and pressure, respectively. In the above equations, ρ represents density, k thermal conductivity, c_p specific heat, and μ viscosity of NF. These properties are related to the NF and the following equations are employed to calculate them

$$\rho = \mathrm{Fi}\rho_{\mathrm{p}} + (1-\mathrm{Fi})\rho_{\mathrm{f}}, \tag{5}$$

$$\rho c_{\mathrm{p}} = (1-\mathrm{Fi})\left(\rho c_{\mathrm{p}}\right)_{\mathrm{f}} + \mathrm{Fi}\left(\rho c_{\mathrm{p}}\right)_{\mathrm{p}}. \tag{6}$$

In the above-mentioned equations, the indices p and f refer to the NPs and the base fluid, respectively. The NF viscosity was calculated using the following equation, which is specific to the Al_2O_3/H_2O NF (Khanafer and Vafai, 2011).

$$\mu = -0.4491 + \frac{28.837}{T} + 0.574Fi - 0.1634Fi^2 + 23.053\frac{Fi^2}{T^2} + 0.0132Fi^3 - 2354.735\frac{Fi}{T^3} + 23.498\frac{Fi^2}{d^2} - 3.0185\frac{Fi^3}{d^2}, \tag{7}$$

where d is the diameter of the NPs in nanometers Fi is the volumetric percentage of the NPs. The relationship of thermal conductivity, which depends on the diameter of the NPs, was as follows (Teng et al., 2010).

$$\frac{k}{k_{\mathrm{f}}} = 0.991 + 0.253(100\omega) - 0.001\,T - 0.002d - 0.189(100\omega)^2 + 6.190 \times 10^{-5}T^2 + 1.317\times 10^{-5}d^2 + 0.049(100\omega)^3 - 7.66\times 10^{-7}T^3, \tag{8}$$

where ω is the mass percentage of NPs, and T is the temperature in degree Celsius. The other properties of the fluid and Al_2O_3 NPs are provided in **Figure 2**.

BOUNDARY CONDITIONS

Figure 3 shows the boundary condition of the problem. The temperature values and boundary conditions at the inlet and outlet of the heat sink are displayed in **Figure 2**. The properties of water and NPs are also present in this figure. A constant flux of 100 W/cm^2 is applied to the bottom of the heat sink as shown. According to **Figure 2**, the upper, front, and left walls of the heat

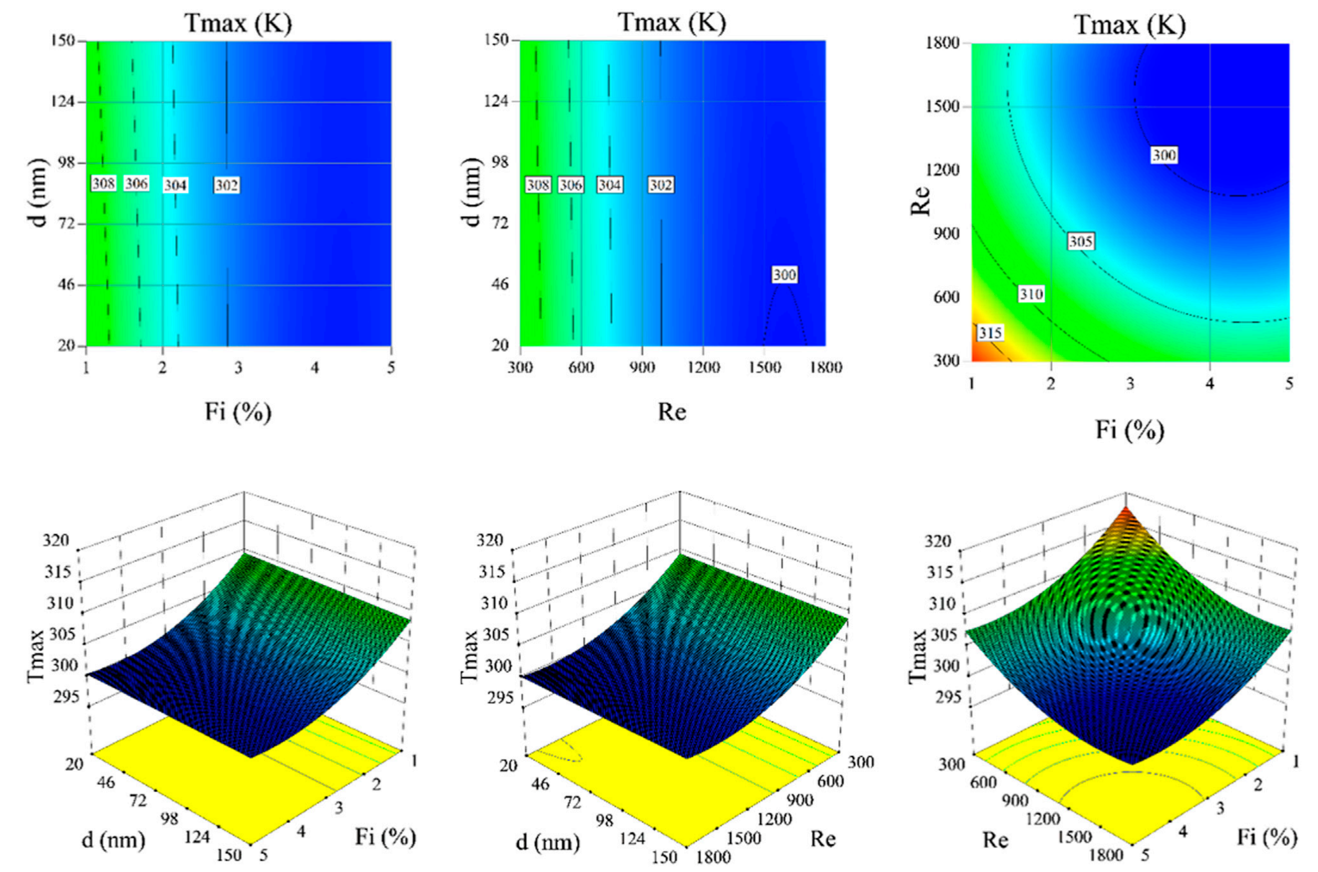

FIGURE 4 | T_{Max} at the bottom of the WMH-S for variations of *Re*, *d*, and *Fi*.

sink are insulated, and the symmetry boundary condition is applied to the back and right walls.

NUMERICAL METHOD AND VALIDATION

For simulating the problem model, its geometry was first drawn in CATIA software. In the next step, the mentioned geometry was transferred to CAMSOL software. Next, an all-hexagonal mesh was applied to the geometry. Then, by entering the properties of NFs and other boundary conditions in this software, the equations were solved and the necessary simulations were performed using the finite element method. The convergence criterion for **Eqs 7–10** is considered. To achieve a proper grid for geometry, many changes were made to the number of elements. Finally it was found that these yield the best results in terms of the solution time as well as the accuracy of the results for the number of 1,550,000 elements. The average temperature changes of the heat sink for the number of different elements are given in **Table 1** in the Re = 300 for 5% nanofluid. The trend of the changes in the heat sink average temperature shows the accuracy of selecting this number of elements.

In order to validate the numerical solution, the results of the present study were compared with some articles, one of which is provided below. Thus, the average Nusselt number obtained from the present work is compared with the experimental work of Ho and Chen (2013) for different channel lengths (**Table 2**). It can be observed that the amount of error between the present results and those reported by Ho and Chen (2013) is less than 4%, indicating that the present simulations are acceptable.

DATA REDUCTION

To assess the thermal performance of the H-S, it was of necessity to investigate parameters such as the heat transfer coefficient (HTC) and the pumping power PP. The convective HTC for the H-S was defined as follows (Bahiraei and Heshmatian, 2017).

$$h = \frac{q''}{T_{Ave} - T_{mid}}. \tag{9}$$

T_{mid} can be obtained using $\frac{T_{in}-T_{out}}{2}$, where T_{in} is the inlet temperature and T_{out} is the outlet temperature. T_{Ave} is also the average temperature of the H-S bottom and q'' represents the thermal flux applied to the WMH-S.

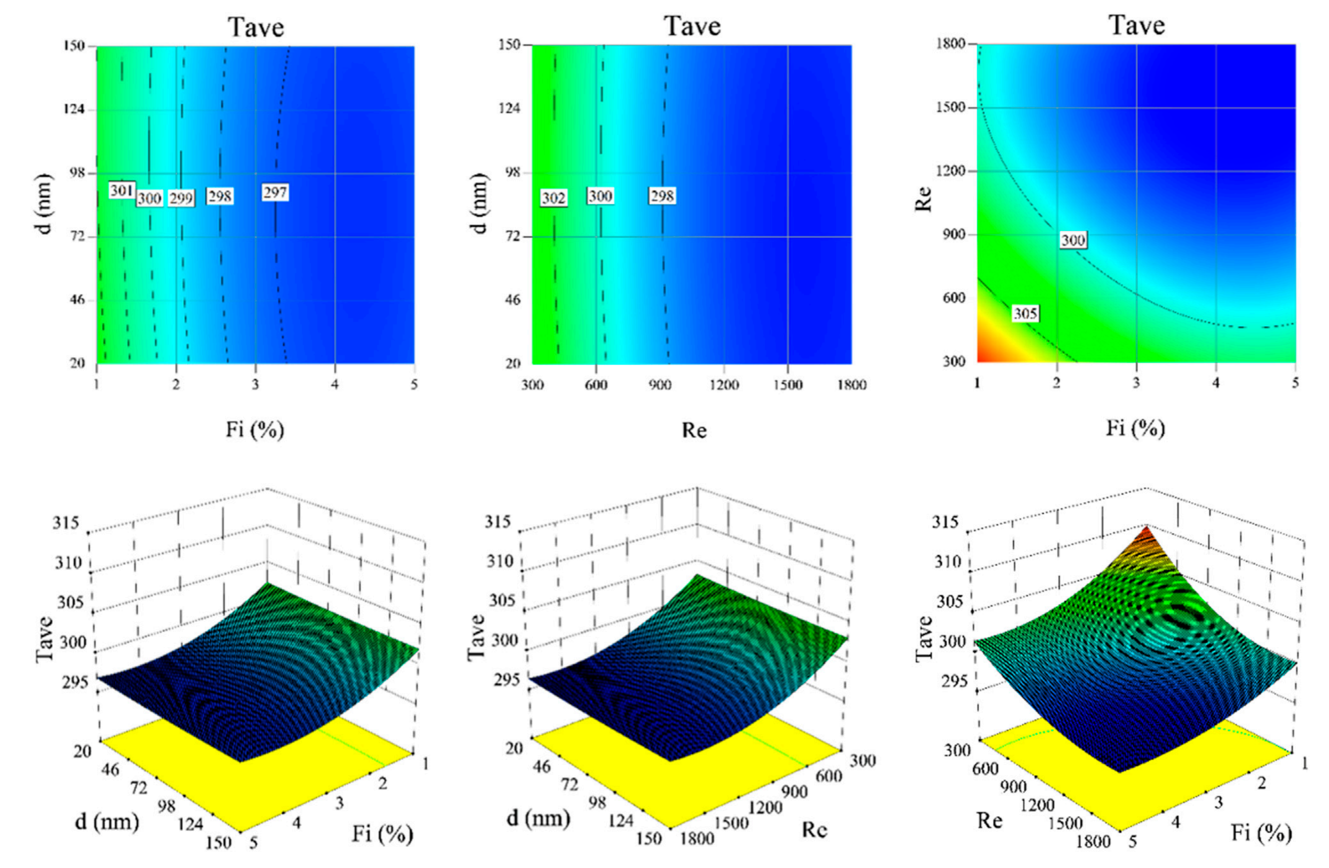

FIGURE 5 | Average temperature of the bottom of the H-S for variations of Re, d, and Fi.

In the following relations, two increased ratios of HTC and PP are introduced.

$$PP = \dot{Q}\Delta P, \tag{10}$$

$$h_{eff} = \frac{(h - h_f)}{h_f} \times 100. \tag{11}$$

In the PP relation, $\dot{Q}$ indicates the volumetric flow rate of the fluid and ΔP is the pressure difference on both sides of the H-S.

Other parameters can also be utilized to measure the thermal performance of H-Ss. Two important parameters in evaluating the performance of H-Ss are the thermal resistance and temperature uniformity, the relationships of which are listed below. The lower the two parameters, the better the performance of H-Ss.

$$R = \frac{T_{Ave} - T_{in}}{q''}, \tag{12}$$

$$Theta = \frac{T_{Max} - T_{Min}}{q''}. \tag{13}$$

In the above equations, the indices Max and Min represent the maximum and minimum temperatures on the lower surface of the H-S.

A parameter that is considered when using NFs in various devices is the figure of merit (FOM), whose relationship is presented below, indicates the ratio of convective HTC of NF to H_2O to the ΔP of NF to H_2O (Bahiraei and Heshmatian, 2017).

$$FOM = \frac{h/h_f}{\Delta P/\Delta P_f}. \tag{14}$$

RESULTS AND DISCUSSION

Figure 3 demonstrated the temperature contour of the WMH-S for H_2O and NF 2% in different *Re*. At low velocities of the fluid, it can be seen that the fluid heated up at the beginning of WMH-S and had a low heat transfer in the end. As the fluid velocity increased, the fluid with lower temperatures moved inside the WMH-S, and as a result, cooling in the end of the WMH-S increased.

Figure 4 shows the T_{Max} at the bottom of the WMH-S for variations of *Re*, *d*, and *Fi*. As it can be observed, an intensification in the *Re* always decreased the T_{Max}. Faster passage of fluid through the WMH-S improved cooling, thus, the heat transfer increased and the WMH-S temperature got closer to the fluid temperature. Hence, the T_{Max} was also decreased. Increasing the Fi also reduced the T_{Max} of the WMH-S. The application of NF resulted in a higher thermal conductivity of the fluid, which increased the heat transfer from the WMH-S to the fluid. Therefore, it lowered the temperature of the

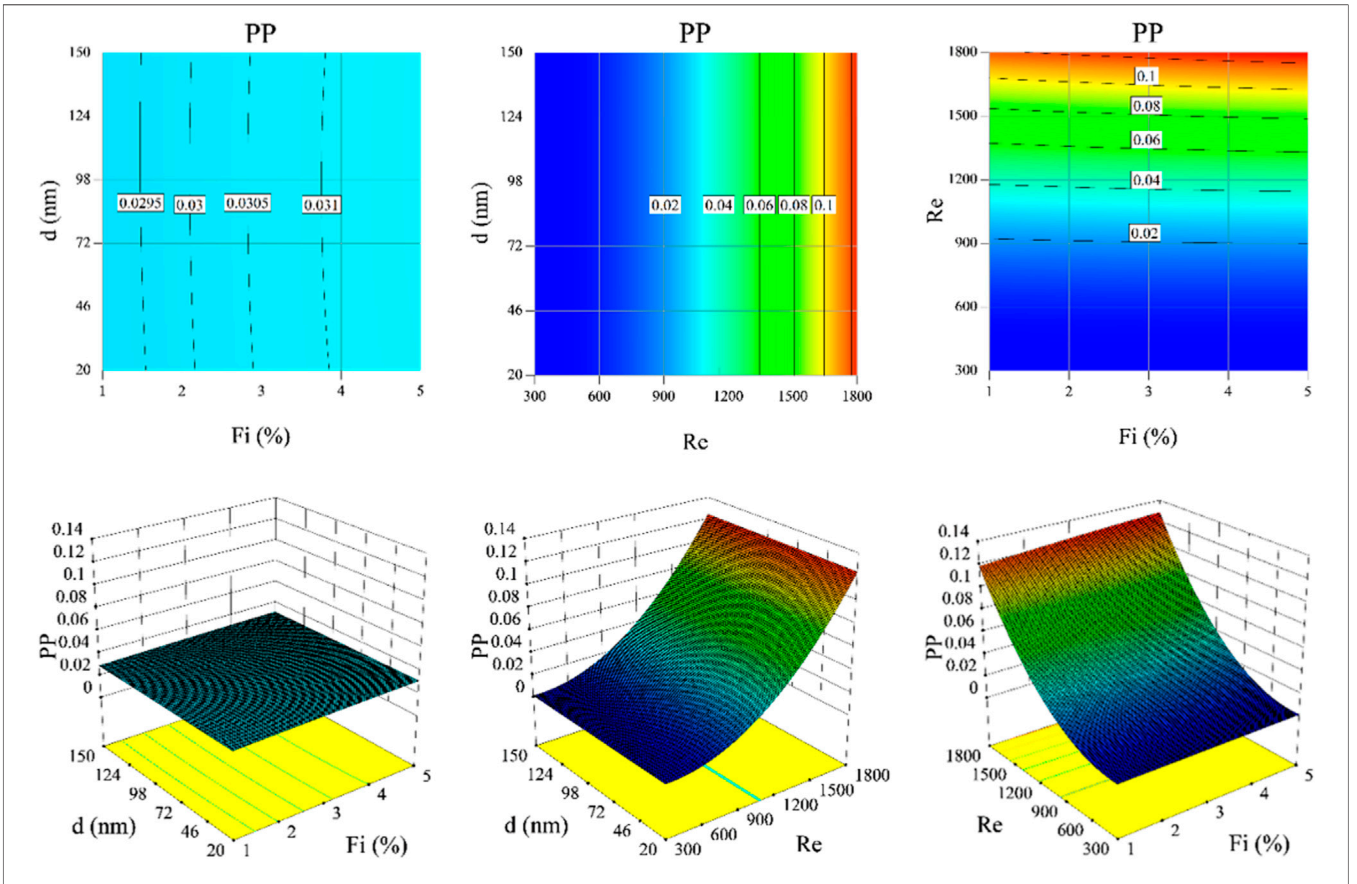

FIGURE 6 | PP required to flow the fluid for dissimilar values of *Re*, *d*, and *Fi*.

WMH-S. In the higher Fi, the T_{Max} obtained using NF containing small-sized NPs was lower, while in the low volume percentage, NF containing large-sized NPs generated lower T_{Max}. Both the viscosity and the thermal conductivity depend on the temperature, the volumetric percentage of the NPs, and the diameter of the NPs; hence, in different volume percentages and temperatures, the effect of NP diameter on the heat transfer could vary.

Figure 5 displays the average temperature of the bottom of the H-S for variations of Re, d, and Fi. As it can also be observed, an intensification in the *Re* diminished the average temperature in the WMH-S and an intensification in the Fi decreased the average temperature. As mentioned above, the increase in these two parameters increased the heat transfer between the WMH-S and the fluid, thus reducing the overall temperature of WMH-S and making its temperature closer to the temperature of the fluid. The changes in the average temperature varied based on the changes in the NP diameter at different volume percentages. Of course, the amount of these changes was far less than the temperature changes with the Fi and Re. The average temperature appeared to be lower in medium-sized NPs, especially at high volumetric percentages.

Figure 6 demonstrated the PP required to flow the fluid for dissimilar values of *Re*, *d*, and *Fi*. The intensification in Re and, consequently, the escalation in fluid velocity greatly increased the PP. Increasing the ΔP, as well as the flow rate by increasing the *Re*, raised the PP. An increase in the Fi also increased this parameter, stemming from the increase in ΔP in the WMH-S. It can be seen that the variations in the PP with the NP diameter were very small; however, in a high-volume percentage, employing smaller NPs resulted in the requirement of less PP. The use of smaller NPs increased the viscosity, and consequently, the shear stress reduced. As a result, the employment of smaller NPs slightly increased PP.

Figure 7 demonstrates the increase percentage in the HTC for different values of *Re*, *d*, and *Fi*. Increasing the *Re* and the Fi always increased the HTC. It was seen that growing the Fi maintained the upward trend of increasing the HTC and always increased it. However, with the intensification of the *Re* in the high volume percentages of NPs, the increase in the HTC was initially low, but in higher *Re*, the increasing trend was steeper and increased significantly; while in the low Fi, the increase in the *Re* always created an increasing trend in the HTC. It was also noticed that in high and low *Re*, the effect of adding NPs was more promising than that in medium *Re*. Furthermore, the increase in the HTC was higher for the average-sized NPs.

Figure 8 demonstrates the temperature uniformity on the bottom of the WMH-S for dissimilar values of *Re, d*, and *Fi*. Here, the intensification in the *Re* and the volumetric percentage of the NPs reduced the *Theta*, indicating that the temperature at the bottom of the WMH-S was uniform. The decrease in temperature

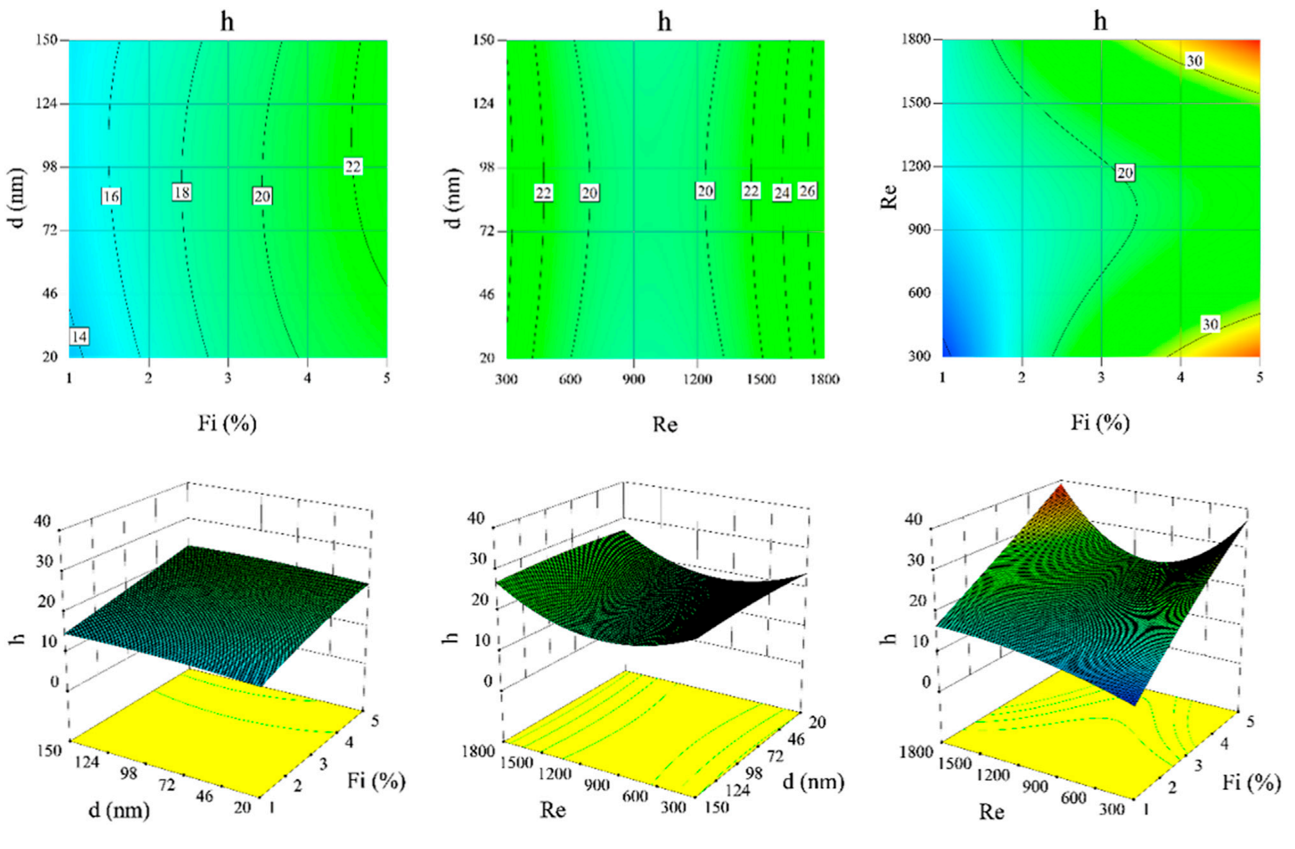

FIGURE 7 | Increase in percentage in the HTC for different values of *Re*, *d*, and *Fi*.

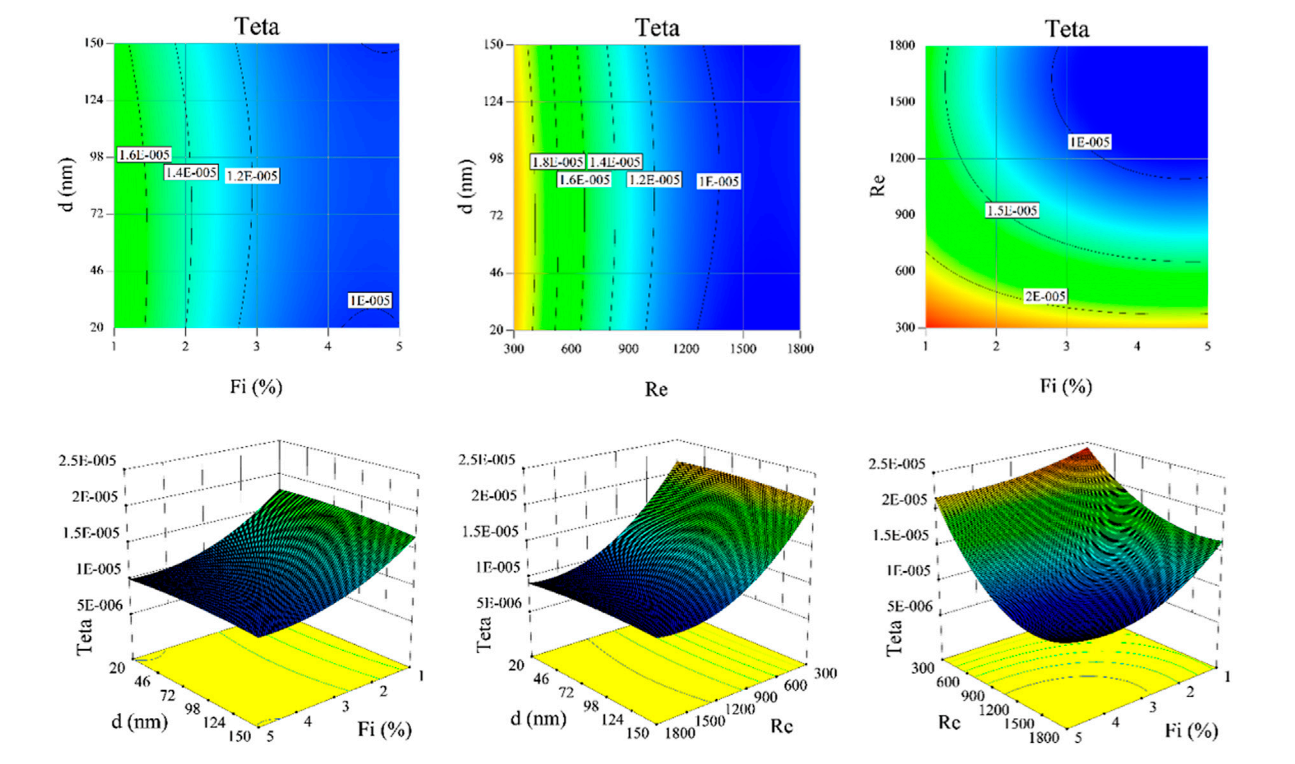

FIGURE 8 | Temperature uniformity on the bottom of the WMH-S for dissimilar values of *Re*, *d*, and *Fi*.

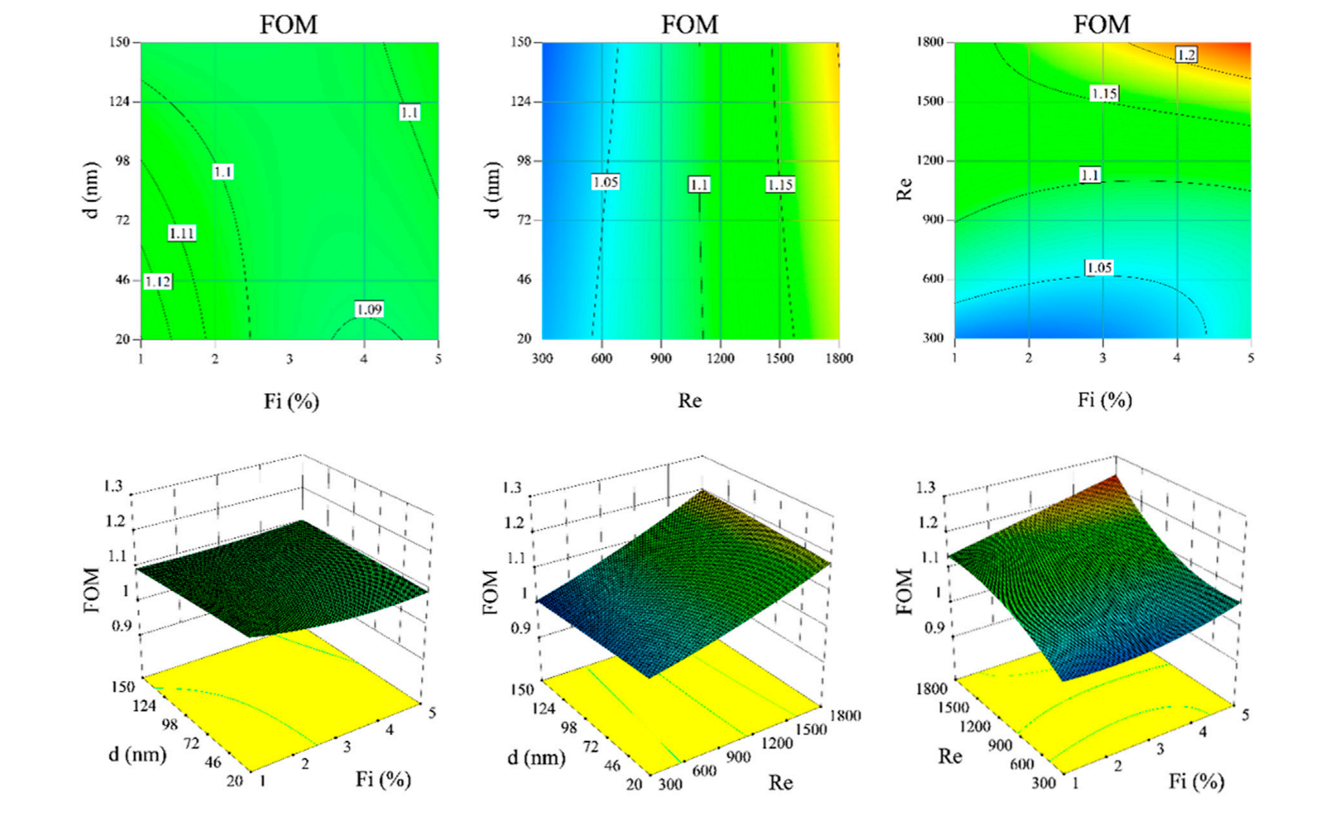

FIGURE 9 | FOM for dissimilar values of *Re*, *d*, and *Fi*.

caused the temperature to be uniform in this part, stemming from better heat transfer between the fluid and the solid walls. In the average diameters of NPs, *Theta* was higher, meaning that the larger diameter of NPs had better temperature uniformity.

Figure 9 shows the FOM for dissimilar values of *Re*, *d*, and *Fi*. The best case for adding NPs in terms of heat transfer to ΔP was in high *Re* such that the highest FOM was approximately 1.25, which occurred in the *Re* of 1800 for 5% of the Fi. In higher *Re*, the increase in HTC was greater than the increase in ΔP; while in lower *Re* (300), the decrease in FOM was less than one, meaning the ratio of increase in ΔP with the addition of NPs was higher than the increase in HTC. Investigating the NP diameter demonstrated that application of NPs with a larger size resulted in a higher FOM.

CONCLUSION

In this article, a new WMH-S with five microchannels was simulated. The walls of the microchannels were wavy. H_2O and Al_2O_3/H_2O NF were employed as the coolant. The model utilized for viscosity and conductivity of the NF was related to the diameter of the NPs. With the changes in the *Re*, the volumetric percentage of the NPs, and their diameters, the thermal performance of the WMH-S was considered and the main obtained results are as follows:

1) Increasing the *Re* and the percentage of NPs reduced the maximum and minimum temperatures at the bottom of the WMH-S.
2) Increasing the diameter of the NPs at a higher Fi increased the T_{Max} of the WMH-S, while those at a low volume percentage reduced it. The addition of nanoparticles reduces the heat sink maximum temperature by 3.8 and 2.5% at the Reynolds numbers of 300 and 1800, respectively.
3) With increasing the *Re* and volume percentage, more PP was required. Thus, the cost of PP also increases.
4) In high percentages of NPs, the increase in the size of NPs also raised the PP.
5) The HTC augmented with increasing *Re* and Fi.
6) The temperature uniformity increased with the intensification of *Re* and the volumetric percentage of NPs, and its thermal resistance decreased.
7) The highest FOM was approximately 1.25, occurring in high *Re*s and volume percentages of NPs.

DATA AVAILABILITY STATEMENT

The original contributions presented in the study are included in the article/Supplementary Material, further inquiries can be directed to the corresponding authors.

AUTHOR CONTRIBUTIONS

All authors wrote the manuscript, provided critical feedback, and helped shape the research, analysis, and manuscript. All authors discussed the results and commented on the manuscript.

FUNDING

This work was supported by the Taif University Researchers Supporting grant number (TURSP-2020/266) of Taif University, Taif, Saudi Arabia.

REFERENCES

Afrand, M., Farahat, S., Nezhad, A. H., Ali Sheikhzadeh, G., and Sarhaddi, F. (2014). 3-D Numerical Investigation of Natural Convection in a Tilted Cylindrical Annulus Containing Molten Potassium and Controlling it Using Various Magnetic fields. *Int. J. Appl. Electromagnetics Mech.* 46, 809–821. doi:10.3233/jae-141975

Ahmadi, A., Arabbeiki, M., Ali, H. M., Goodarzi, M., and Safaei, M. R. (2020). Configuration and Optimization of a Minichannel Using Water–Alumina Nanofluid by Non-dominated Sorting Genetic Algorithm and Response Surface Method. *Nanomaterials (Basel)* 10 (5), 901. doi:10.3390/nano10050901

Ahmadi, M. H., Mohseni-Gharyehsafa, B., Ghazvini, M., Goodarzi, M., Jilte, R. D., and Kumar, R. (2020). Comparing Various Machine Learning Approaches in Modeling the Dynamic Viscosity of CuO/water Nanofluid. *J. Therm. Anal. Calorim.* 139 (4), 2585–2599. doi:10.1007/s10973-019-08762-z

Ahmed, H. E., Salman, B. H., Kherbeet, A. S., and Ahmed, M. I. (2018). Optimization of thermal Design of Heat Sinks: A Review. *Int. J. Heat Mass Transfer* 118, 129–153. doi:10.1016/j.ijheatmasstransfer.2017.10.099

Akbari, M., Galanis, N., and Behzadmehr, A. (2011). Comparative Analysis of Single and Two-phase Models for CFD Studies of Nanofluid Heat Transfer. *Int. J. Therm. Sci.* 50 (8), 1343–1354. doi:10.1016/j.ijthermalsci.2011.03.008

Alfaryjat, A. A., Mohammed, H. A., Adam, N. M., Stanciu, D., and Dobrovicescu, A. (2018). Numerical Investigation of Heat Transfer Enhancement Using Various Nanofluids in Hexagonal Microchannel Heat Sink. *Therm. Sci. Eng. Prog.* 5, 252–262. doi:10.1016/j.tsep.2017.12.003

Alihosseini, Y., Zabetian Targhi, M., Heyhat, M. M., and Ghorbani, N. (2020). Effect of a Micro Heat Sink Geometric Design on Thermo-Hydraulic Performance: A Review. *Appl. Therm. Eng.* 170, 114974. doi:10.1016/j.applthermaleng.2020.114974

Ambreen, T., and Kim, M.-H. (2020). Influence of Particle Size on the Effective thermal Conductivity of Nanofluids: A Critical Review. *Appl. Energ.* 264, 114684. doi:10.1016/j.apenergy.2020.114684

Arani, A. A. A., Sadripour, S., and Kermani, S. (2017). Nanoparticle Shape Effects on thermal-hydraulic Performance of Boehmite Alumina Nanofluids in a Sinusoidal-Wavy Mini-Channel with Phase Shift and Variable Wavelength. *Int. J. Mech. Sci.* 128-129, 550–563. doi:10.1016/j.ijmecsci.2017.05.030

Awais, A. A., and Kim, M.-H. (2020). Experimental and Numerical Study on the Performance of a Minichannel Heat Sink with Different Header Geometries Using Nanofluids. *Appl. Therm. Eng.* 171, 115125. doi:10.1016/j.applthermaleng.2020.115125

Aybar, H. Ş., Sharifpur, M., Azizian, M. R., Mehrabi, M., and Meyer, J. P. (2015). A Review of Thermal Conductivity Models for Nanofluids. *Heat Transfer Eng.* 36 (13), 1085–1110. doi:10.1080/01457632.2015.987586

Bagherzadeh, S. A., D'Orazio, A., Karimipour, A., Goodarzi, M., and Bach, Q.-V. (2019). A Novel Sensitivity Analysis Model of EANN for F-MWCNTs-Fe3O4/EG Nanofluid thermal Conductivity: Outputs Predicted Analytically Instead of Numerically to More Accuracy and Less Costs. *Physica A: Stat. Mech. its Appl.* 521, 406–415. doi:10.1016/j.physa.2019.01.048

Bahiraei, M., and Heshmatian, S. (2017). Application of a Novel Biological Nanofluid in a Liquid Block Heat Sink for Cooling of an Electronic Processor: Thermal Performance and Irreversibility Considerations. *Energ. Convers. Manage.* 149, 155–167. doi:10.1016/j.enconman.2017.07.020

Bahiraei, M., and Heshmatian, S. (2018). Electronics Cooling with Nanofluids: A Critical Review. *Energ. Convers. Manage.* 172, 438–456. doi:10.1016/j.enconman.2018.07.047

Bahiraei, M., and Heshmatian, S. (2018). Thermal Performance and Second Law Characteristics of Two New Microchannel Heat Sinks Operated with Hybrid Nanofluid Containing Graphene-Silver Nanoparticles. *Energ. Convers. Manage.* 168, 357–370. doi:10.1016/j.enconman.2018.05.020

Bahrami, M., Akbari, M., Bagherzadeh, S. A., Karimipour, A., Afrand, M., and Goodarzi, M. (2019). Develop 24 Dissimilar ANNs by Suitable Architectures & Training Algorithms via Sensitivity Analysis to Better Statistical Presentation: Measure MSEs between Targets & ANN for Fe-CuO/Eg-Water Nanofluid. *Physica A: Stat. Mech. its Appl.* 519, 159–168. doi:10.1016/j.physa.2018.12.031

Esfe, M. H., Esfandeh, S., Afrand, M., Rejvani, M., and Rostamian, S. H. (2018). Experimental Evaluation, New Correlation Proposing and ANN Modeling of thermal Properties of EG Based Hybrid Nanofluid Containing ZnO-DWCNT Nanoparticles for Internal Combustion Engines Applications. *Appl. Therm. Eng.* 133, 452–463. doi:10.1016/j.applthermaleng.2017.11.131

Ghalandari, M., Maleki, A., Haghighi, A., Safdari Shadloo, M., Alhuyi Nazari, M., and Tlili, I. (2020). Applications of Nanofluids Containing Carbon Nanotubes in Solar Energy Systems: A Review. *J. Mol. Liquids* 313, 113476. doi:10.1016/j.molliq.2020.113476

Ghani, I. A., Sidik, N. A. C., and Kamaruzaman, N. (2017). Hydrothermal Performance of Microchannel Heat Sink: The Effect of Channel Design. *Int. J. Heat Mass Transfer* 107, 21–44. doi:10.1016/j.ijheatmasstransfer.2016.11.031

Ghodsinezhad, H., Sharifpur, M., and Meyer, J. P. (2016). Experimental Investigation on Cavity Flow Natural Convection of Al 2 O 3 -water Nanofluids. *Int. Commun. Heat Mass Transfer* 76, 316–324. doi:10.1016/j.icheatmasstransfer.2016.06.005

Giwa, S. O., Sharifpur, M., Goodarzi, M., Alsulami, H., and Meyer, J. P. (2021). Influence of Base Fluid, Temperature, and Concentration on the Thermophysical Properties of Hybrid Nanofluids of Alumina–Ferrofluid: Experimental Data, Modeling through Enhanced ANN, ANFIS, and Curve Fitting. *J. Therm. Anal. Calorim.* 143 (6), 4149–4167. doi:10.1007/s10973-020-09372-w

Guan, H., Huang, S., Ding, J., Tian, F., Xu, Q., and Zhao, J. (2020). Chemical Environment and Magnetic Moment Effects on point Defect Formations in CoCrNi-Based Concentrated Solid-Solution Alloys. *Acta Materialia* 187, 122–134. doi:10.1016/j.actamat.2020.01.044

Hajatzadeh Pordanjani, A., Aghakhani, S., Afrand, M., Mahmoudi, B., Mahian, O., and Wongwises, S. (2019). An Updated Review on Application of Nanofluids in Heat Exchangers for Saving Energy. *Energ. Convers. Manage.* 198, 111886. doi:10.1016/j.enconman.2019.111886

Handschuh-Wang, S., Wang, T., and Tang, Y. (2021). Ultrathin Diamond Nanofilms—Development, Challenges, and Applications. *Small* 17 (30), 2007529. doi:10.1002/smll.202007529

Hemmat Esfe, M., Rostamian, H., Esfandeh, S., and Afrand, M. (2018). Modeling and Prediction of Rheological Behavior of Al2O3-Mwcnt/5w50 Hybrid Nano-Lubricant by Artificial Neural Network Using Experimental Data. *Physica A: Stat. Mech. its Appl.* 510, 625–634. doi:10.1016/j.physa.2018.06.041

Ho, C. J., and Chen, W. C. (2013). An Experimental Study on thermal Performance of Al2O3/water Nanofluid in a Minichannel Heat Sink. *Appl. Therm. Eng.* 50 (1), 516–522. doi:10.1016/j.applthermaleng.2012.07.037

Hu, P., Cao, L., Su, J., Li, Q., and Li, Y. (2020). Distribution Characteristics of Salt-Out Particles in Steam Turbine Stage. *Energy* 192, 116626. doi:10.1016/j.energy.2019.116626

Hu, Y., Qing, J. x., Liu, Z. H., Conrad, Z. J., Cao, J. N., and Zhang, X. P. (2021). Hovering Efficiency Optimization of the Ducted Propeller with Weight Penalty Taken into Account. *Aerospace Sci. Technol.* 117, 106937. doi:10.1016/j.ast.2021.106937

Irandoost Shahrestani, M., Maleki, A., Safdari Shadloo, M., and Tlili, I. (2020). Numerical Investigation of Forced Convective Heat Transfer and Performance Evaluation Criterion of Al2O3/Water Nanofluid Flow inside an. *Axisymmetric Microchannel* 12 (1), 120. doi:10.3390/sym12010120

Kalbasi, R., Afrand, M., Alsarraf, J., and Tran, M.-D. (2019). Studies on Optimum Fins Number in PCM-Based Heat Sinks. *Energy* 171, 1088–1099. doi:10.1016/j.energy.2019.01.070

Kant, K., Shukla, A., Sharma, A., and Henry Biwole, P. (2017). Heat Transfer Study of Phase Change Materials with Graphene Nano Particle for thermal Energy Storage. *Solar Energy* 146, 453–463. doi:10.1016/j.solener.2017.03.013

Khanafer, K., and Vafai, K. (2011). A Critical Synthesis of Thermophysical Characteristics of Nanofluids. *Int. J. Heat Mass Transfer* 54 (19), 4410–4428. doi:10.1016/j.ijheatmasstransfer.2011.04.048

Kumar, S., Kumar, A., Darshan Kothiyal, A., and Singh Bisht, M. (2018). A Review of Flow and Heat Transfer Behaviour of Nanofluids in Micro Channel Heat Sinks. *Therm. Sci. Eng. Prog.* 8, 477–493. doi:10.1016/j.tsep.2018.10.004

Kumar, S., and Singh, P. K. (2019). A Novel Approach to Manage Temperature Non-uniformity in Minichannel Heat Sink by Using Intentional Flow Maldistribution. *Appl. Therm. Eng.* 163, 114403. doi:10.1016/j.applthermaleng.2019.114403

Mohammed Adham, A., Mohd-Ghazali, N., and Ahmad, R. (2013). Thermal and Hydrodynamic Analysis of Microchannel Heat Sinks: A Review. *Renew. Sustain. Energ. Rev.* 21, 614–622. doi:10.1016/j.rser.2013.01.022

Nguyen, T. K., Saidizad, A., Jafaryar, M., Sheikholeslami, M., Barzegar Gerdroodbary, M., Moradi, R., et al. (2019). Influence of Various Shapes of CuO Nanomaterial on Nanofluid Forced Convection within a Sinusoidal Channel with Obstacles. *Chem. Eng. Res. Des.* 146, 478–485. doi:10.1016/j.cherd.2019.04.030

Osman, S., Sharifpur, M., and Meyer, J. P. (2019). Experimental Investigation of Convection Heat Transfer in the Transition Flow Regime of Aluminium Oxide-Water Nanofluids in a Rectangular Channel. *Int. J. Heat Mass Transfer* 133, 895–902. doi:10.1016/j.ijheatmasstransfer.2018.12.169

Peng, Y., Parsian, A., Khodadadi, H., Akbari, M., Ghani, K., Goodarzi, M., et al. (2020). Develop Optimal Network Topology of Artificial Neural Network (AONN) to Predict the Hybrid Nanofluids thermal Conductivity According to the Empirical Data of Al2O3 - Cu Nanoparticles Dispersed in Ethylene Glycol. *Physica A: Stat. Mech. its Appl.* 549, 124015. doi:10.1016/j.physa.2019.124015

Pordanjani, A. H., Aghakhani, S., Afrand, M., Sharifpur, M., Meyer, J. P., Xu, H., et al. (2021). Nanofluids: Physical Phenomena, Applications in thermal Systems and the Environment Effects- a Critical Review. *J. Clean. Prod.* 320, 128573. doi:10.1016/j.jclepro.2021.128573

Pordanjani, A. H., and Aghakhani, S. (2021). Numerical Investigation of Natural Convection and Irreversibilities between Two Inclined Concentric Cylinders in Presence of Uniform Magnetic Field and Radiation. *Heat Transfer Eng.* 43 (11), 1–21. doi:10.1080/01457632.2021.1919973

Pordanjani, A. H., Raisi, A., and Ghasemi, B. (2019). Numerical Simulation of the Magnetic Field and Joule Heating Effects on Force Convection Flow through Parallel-Plate Microchannel in the Presence of Viscous Dissipation Effect. *Numer. Heat Transfer, A: Appl.* 76, 1–18. doi:10.1080/10407782.2019.1642053

Safdari Shadloo, M. (2021). Application of Support Vector Machines for Accurate Prediction of Convection Heat Transfer Coefficient of Nanofluids through Circular Pipes. *Int. J. Numer. Methods Heat Fluid Flow* 31 (8), 2660–2679. doi:10.1108/hff-09-2020-0555

Shadloo, M. S., Rahmat, A., Karimipour, A., and Wongwises, S. (2020). Estimation of Pressure Drop of Two-phase Flow in Horizontal Long Pipes Using Artificial Neural Networks. *J. Energ. Resour. Technol.* 142 (11), 112110. doi:10.1115/1.4047593

Shalchi-Tabrizi, A., and Seyf, H. R. (2012). Analysis of Entropy Generation and Convective Heat Transfer of Al_2O_3 Nanofluid Flow in a Tangential Micro Heat Sink. *Int. J. Heat Mass Transfer* 55 (15), 4366–4375. doi:10.1016/j.ijheatmasstransfer.2012.04.005

Sharifpur, M., Yousefi, S., and Meyer, J. P. (2016). A New Model for Density of Nanofluids Including Nanolayer. *Int. Commun. Heat Mass Transfer* 78, 168–174. doi:10.1016/j.icheatmasstransfer.2016.09.010

Sohel, M. R., Saidur, R., Khaleduzzaman, S. S., and Ibrahim, T. A. (2015). Cooling Performance Investigation of Electronics Cooling System Using Al2O3-H2o Nanofluid. *Int. Commun. Heat Mass Transfer* 65, 89–93. doi:10.1016/j.icheatmasstransfer.2015.04.015

Sohel Murshed, S. M., and Nieto de Castro, C. A. (2017). A Critical Review of Traditional and Emerging Techniques and Fluids for Electronics Cooling. *Renew. Sustain. Energ. Rev.* 78, 821–833. doi:10.1016/j.rser.2017.04.112

Sokhal, G. S., Dhindsa, G. S., Sokhal, K. S., Ghazvini, M., Sharifpur, M., and Sadeghzadeh, M. (2021). Experimental Investigation of Heat Transfer and Exergy Loss in Heat Exchanger with Air Bubble Injection Technique. *J. Therm. Anal. Calorim.* 145, 727. doi:10.1007/s10973-020-10192-1

Teng, T.-P., Hung, Y.-H., Teng, T.-C., Mo, H.-E., and Hsu, H.-G. (2010). The Effect of Alumina/water Nanofluid Particle Size on thermal Conductivity. *Appl. Therm. Eng.* 30 (14), 2213–2218. doi:10.1016/j.applthermaleng.2010.05.036

Tian, M.-W., Rostami, S., Aghakhani, S., Goldanlou, A. S., and Qi, C. (2021). A Techno-Economic Investigation of 2D and 3D Configurations of Fins and Their Effects on Heat Sink Efficiency of MHD Hybrid Nanofluid with Slip and Non-slip Flow. *Int. J. Mech. Sci.* 189, 105975. doi:10.1016/j.ijmecsci.2020.105975

Toghyani, S., Afshari, E., Baniasadi, E., and Shadloo, M. S. (2019). Energy and Exergy Analyses of a Nanofluid Based Solar Cooling and Hydrogen Production Combined systemEnergy and Exergy Analyses of a Nanofluid Based Solar Cooling and Hydrogen Production Combined System. *Renew. Energ.* 141, 1013–1025. doi:10.1016/j.renene.2019.04.073

Tullius, J. F., Vajtai, R., and Bayazitoglu, Y. (2011). A Review of Cooling in Microchannels. *Heat Transfer Eng.* 32 (7-8), 527–541. doi:10.1080/01457632.2010.506390

Vahedi, S. M., Pordanjani, A. H., Raisi, A., and Chamkha, A. J. (2019). Sensitivity Analysis and Optimization of MHD Forced Convection of a Cu-Water Nanofluid Flow Past a Wedge. *The Eur. Phys. J. Plus* 134 (3), 124. doi:10.1140/epjp/i2019-12537-x

Wang, X., Handschuh-Wang, S., Xu, Y., Xiang, L., Zhou, Z., Wang, T., et al. (2021). Hierarchical Micro/Nanostructured Diamond Gradient Surface for Controlled Water Transport and Fog Collection. *Adv. Mater. Inter.* 8 (12), 2100196. doi:10.1002/admi.202100196

Wu, J., Zhao, J., Lei, J., and Liu, B. (2016). Effectiveness of Nanofluid on Improving the Performance of Microchannel Heat Sink. *Appl. Therm. Eng.* 101, 402–412. doi:10.1016/j.applthermaleng.2016.01.114

Yan, S.-R., Aghakhani, S., and Karimipour, A. (2020). Influence of a Membrane on Nanofluid Heat Transfer and Irreversibilities inside a Cavity with Two Constant-Temperature Semicircular Sources on the Lower wall: Applicable to Solar Collectors. *Physica Scripta* 95 (8), 085702. doi:10.1088/1402-4896/ab93e4

Zhang, X., Sun, X., Lv, T., Weng, L., Chi, M., Shi, J., et al. (2020). Preparation of PI Porous Fiber Membrane for Recovering Oil-Article Insulation Structure. *J. Mater. Sci. Mater. Electron.* 31 (16), 13344–13351. doi:10.1007/s10854-020-03888-5

Zheng, Y., Yaghoubi, S., Dezfulizadeh, A., Aghakhani, S., Karimipour, A., and Tlili, I. (2020). Free Convection/radiation and Entropy Generation Analyses for Nanofluid of Inclined Square Enclosure with Uniform Magnetic Field. *J. Therm. Anal. Calorim.* 141 (1), 635–648. doi:10.1007/s10973-020-09497-y

Conflict of Interest: The authors declare that the research was conducted in the absence of any commercial or financial relationships that could be construed as a potential conflict of interest.